

Article

# 3,4-DHPEA-EA Peracetylated (3,4-DHPEA-EA(P)) Attenuates H<sub>2</sub>O<sub>2</sub>-Mediated Cytotoxicity in C2C12 Myocytes *via* Inactivation of p-JNK/p-c-Jun Signaling Pathway

Monica Nardi<sup>1\*</sup>, Sara Baldelli<sup>2\*</sup>, Maria Rosa Ciriolo<sup>3,4</sup>, Carmela Colica<sup>5</sup>, Paola Costanzo<sup>1</sup> and Antonio Procopio<sup>1</sup>

<sup>1</sup> Dipartimento di Scienze della Salute, Università Magna Graecia, Viale Europa, 88100-Germaneto (CZ), Italy; [monica.nardi@unicz.it](mailto:monica.nardi@unicz.it) (M.N.); [pcostanzo@unicz.it](mailto:pcostanzo@unicz.it) (P.C.); [procopio@unicz.it](mailto:procopio@unicz.it) (A.P.)

<sup>2</sup> Department of Human Sciences and Promotion of the Quality of Life, IRCCS San Raffaele Pisana, San Raffaele Roma Open University, Rome, Italy, [sara.baldellil@uniroma5.it](mailto:sara.baldellil@uniroma5.it) (S.B.)

<sup>3</sup> University of Rome "Tor Vergata", Department of Biology, Rome, Italy; [ciriolo@bio.uniroma2.it](mailto:ciriolo@bio.uniroma2.it) (M.R.C.)

<sup>4</sup> IRCCS San Raffaele Pisana, Rome, Italy

<sup>5</sup> CNR, IBFM UOS, Università Magna Graecia, Viale Europa, 88100-Germaneto (CZ), Italy; [carmela.colica@cnr.it](mailto:carmela.colica@cnr.it) (C.C.)

\* Correspondence: ; [monica.nardi@unicz.it](mailto:monica.nardi@unicz.it); Tel.: +39-0961-3694116 (M.N.); [sara.baldellil@uniroma5.it](mailto:sara.baldellil@uniroma5.it); Tel.: +39-0672-514366 (S.B.)

**Abstract:** Oleuropein, glycosylated secoiridoid present in the olive leaves, is known as an important antioxidant phenolic compound. We studied the antioxidant effect of low dose of oleuropein aglycone (3,4-DHPEA-EA) and oleuropein aglycone peracetylated (3,4-DHPEA-EA(P)) in murine C2C12 myocytes treated with hydrogen peroxide (H<sub>2</sub>O<sub>2</sub>). Both compounds were used at a concentration of 10 μM and were able to inhibit cell death induced by H<sub>2</sub>O<sub>2</sub> treatment, with 3,4-DHPEA-EA(P) being more. Under our experimental conditions H<sub>2</sub>O<sub>2</sub> efficiently induced the phosphorylated-active form of JNK and of its downstream target c-Jun. We demonstrated, by Western blot analysis, that 3,4-DHPEA-EA(P) was efficient in inhibiting the phospho-active form of JNK. This data suggest that growth arrest and cell dead of C2C12 proceeds *via* the JNK/c-Jun pathway. Moreover, we demonstrated that 3,4-DHPEA-EA(P) affects myogenesis of C2C12 cells; because the MyoD mRNA levels and the differentiation process are restored after treatment with 3,4-DHPEA-EA(P). Overall, the results indicate that 3,4-DHPEA-EA(P) prevents ROS-mediated degenerative process by functioning as an efficient antioxidant.

**Keywords:** 3,4-DHPEA-EA; C2C12 myocytes; olive oil; antioxidant; skeletal muscle

## 1. Introduction

Oleuropein is the main phenolic compounds of olive leaves and an important bioactive compound with various biological properties including anticancer [1], antidiabetic and antiatherosclerotic [2]. Moreover, several *in vitro* and *in vivo* studies indicate that oleuropein is a potent superoxide anion and other reactive oxygen species (ROS) scavenger [3].

Among the oleuropein derivatives, its aglycone (3,4-DHPEA-EA), a hydrolysis product of oleuropein, it has been shown to have important biological functions among which: to reduce lung inflammation in a mouse-model of carrageenan-induced pleurisy [4], to reduce the plasma levels of pro-inflammatory cytokines, ameliorating the development of collagen-induced arthritis [5] and to improve function protecting against Aβ deposition [6]. It has also been shown that semisynthetic peracetylated oleuropein and its peracetylated derivatives, improved the capacity to permeate the

cell membrane, with enhanced biological activity [2, 7]. Furthermore, it was reported that peracetylation of oleuropein improve not only its affinity to fatty matrix food, such as EVOO oil, but also the stability of the acetylation of oleuropein over time after enrichment [8].

In last years, the importance of the antioxidant activity of 3,4-DHPEA-EA[9-11] and its derivatives at the level of skeletal muscle has emerged [12-14]. Skeletal muscle is a tissue in which ROS play particular importance: at low concentrations ROS act as signaling molecules in signal transduction pathways; instead at high concentrations they can result in oxidative stress and muscular atrophy [15]. In this context, many natural molecules have been tested for their antioxidant properties and ability to reduce the oxidative damage due to ROS production in skeletal muscle [16]. Indeed, pathophysiological conditions such as sarcopenia, muscular atrophy and strenuous exercise are characterized by an increase in radicals [17-19], which can be buffered or prevented through the use of natural antioxidant molecules such as resveratrol [20] and plant extracts [21].

Among the natural molecules 3,4-DHPEA-EA and its derivatives seem to play an important role in regulation of skeletal muscle homeostasis [12, 13]. In particular, it has been demonstrated that oleuropein induces an increase of glucose uptake through the activation of AMP-activated protein kinase (AMPK) and consequent increase in GLUT4 translocation at the cell membrane [13, 22]. Oleuropein also prevents palmitic acid-induced myocellular insulin resistance suggesting the possibility for this molecule to be effective for type 2 diabetes by reducing insulin resistance in skeletal muscles [12]. Moreover, it has been shown that derivatives of oleuropein reduce high fat diet-induced lipid deposits in liver and skeletal muscle, enhance antioxidant enzyme activities, normalize expression of mitochondrial complex subunits and eventually inhibit apoptosis activation [23, 24]. Despite such evidence, the molecular mechanism(s) that characterize and mediate the activity of oleuropein derivatives in skeletal muscle in conditions of homeostasis or after alteration of the redox state as well as during muscular atrophy are currently poorly addressed. Thus, in this study, we characterized the antioxidant effect of low dose of aglycone peracetylated (3,4-DHPEA-EA(P)) in murine C2C12 myocytes treated with hydrogen peroxide ( $H_2O_2$ ). We demonstrated that the cytotoxic effects of  $H_2O_2$  on myocytes viability and myogenesis proceeds *via* activation of p-JNK-p-c-Jun pathway and that it is abolished by 3,4-DHPEA-EA(P) treatment.

## 2. Materials and Methods

### 2.1 Cell cultures and treatments

The murine skeletal muscle C2C12 cells were obtained from the European Collection of Cell Cultures (Salisbury, UK). C2C12 myocytes were cultured in growth medium composed of Dulbecco's Modified Eagle's Medium (DMEM) supplemented with 10% fetal bovine serum (FBS), 100 U/ml penicillin/streptomycin and 2 mM glutamine (Lonza Sales, Basel, Switzerland) and maintained at 37°C in an atmosphere of 5%  $CO_2$  in air. C2C12 myocytes were plated at 80% of confluence and cultured in growth medium for 24 h. To induce differentiation, cells were washed in PBS and growth medium was replaced with differentiation medium (DM), which contained 2% heat inactivated horse serum (Lonza, ECS0090D) for 2 days [25].

Treatments with  $H_2O_2$  were performed with different concentrations ranging from 20 to 100  $\mu M$  after the change with DM (at day 2 of differentiation). The concentration of 100  $\mu M$   $H_2O_2$  was selected for all of the experiments as it gave the most significant degree of cell growth arrest. 3,4-DHPEA-EA and the peracetylated derivative, 3,4-DHPEA-EA(P) were used at a concentration of 10  $\mu M$  (1 h before  $H_2O_2$  treatment) and maintained throughout the experiment. As control, equal amount of DMSO (0.1%) was added to untreated cells. In the indicated experiments catalase was added 1 h prior  $H_2O_2$  treatment at the concentration of 1  $\mu M$  and maintained throughout the experiment.

### 2.2 Analysis of cell viability and proliferation

Adherent (after trypsinization) and detached cells were combined, washed with PBS and directly counted by optical microscope on hemocytometer after Trypan Blue staining. Alternatively,

cell proliferation was measured by using a MTS assay kit “Cell Titer 96® Aqueous One Solution Cell Proliferation assay” (Promega) according to the manufacturer's instructions. Cell proliferation was also assayed by a “Cell Proliferation kit” (Buckinghamshire, UK) based on the immunocytochemical detection of 5-bromo-2'-deoxyuridine (BrdU) incorporated into cellular DNA of proliferating cells. Cells were stained as previously described [26].

### 2.3 RT-qPCR analysis

Total RNA was extracted using TRI Reagent (Sigma-Aldrich) and used for retro-transcription. qPCR was performed in triplicate by using validated qPCR primers (BLAST), Ex TAq qPCR Premix (Lonza Sales) and the Roche Real Time PCR LightCycler II (Roche Applied Science, Monza, Italy). mRNA levels were normalized to RPL, and the relative mRNA levels were determined by using the  $2^{-\Delta\Delta Ct}$  method [27]. The primer sequences are listed in Table 1.

**Table 1.** List of primers used for RT-qPCR analysis.

Genes	Sequences
mMyoD FW	5'-GGGGCCGCTGTAATCCATCATGC-3'
mMyoD RV	5'-GGAGATCCTGCGCAACGCCA-3'
mAtrogin-1 FW	5'-GCGACCTTCCCCAACGCCTG-3'
mAtrogin-1 RV	5'-GGCGACCGGGACAAGAGTGG-3'
mMurf-1 FW	5'-AGGGGCTACCTTCCTCTAAGTG-3'
mMurf-1 RV	5'-TCTTCCCCAGCTGGCAGCCC-3'
mRPL FW	5'-GTACGACCACCACCTTCCGGC-3'
mRPL RV	5'-ATGGCGGAGGGGCAGGTTCTG-3'

### 2.4 Preparation of cell lysates and Western blot analyses

Cell pellets were resuspended in RIPA buffer (50 mM Tris-HCl, pH 8.0, 150 mM NaCl, 12 mM deoxycholic acid, 0.5% Nonidet P-40 and protease inhibitors). Protein samples were used for SDS-PAGE followed by Western blotting as previously described [28]. Nitrocellulose membranes were stained with primary antibodies against Tubulin (1:1000), p-H2A.x (1:1000), p-JNK (1:1000), JNK (1:1000), p-c-Jun (1:1000). Afterward, the membranes were incubated with the appropriate horseradish peroxidase conjugated secondary antibody, and immunoreactive bands were detected by a Fluorchem Imaging System upon staining with ECL Select Western Blotting Detection Reagent (GE Healthcare, Pittsburgh, PA, USA; RPN2235). Immunoblots reported in the figures are representative of at least four experiments that gave similar results. Tubulin was used as loading control.

Proteins were assayed by the method of Lowry [29].

### 2.5 Determination of ROS

ROS were detected by cytofluorimetric analysis after incubation for 1 h before the end of the experiments, at 37°C with 50  $\mu$ M DCF-DA. After treatment, cells were scraped, washed and resuspended in PBS. The fluorescence intensities of 10,000 cells from each sample were detected by FACScalibur instrument (Beckton and Dickinson, San José, CA). Data were analyzed using the WinMDI 2.8 software.

### 2.6 Statistical analysis

The results are presented as means  $\pm$  S.D. Statistical evaluation was conducted by ANOVA, followed by the post hoc Student–Newman–Keuls. Differences were considered to be significant at  $p < 0.05$ .

### 2.7 Synthesis of 3,4-DHPEA-EA and 3,4-DHPEA-EA (P)

3,4-DHPEA-EA methyl-4-(2-(3,4-dihydroxyphenethoxy)-2-oxoethyl)-3-formyl-2-methyl-3,4-dihydro-2H-pyran-5-carboxylate) was obtained by catalytic hydrolysis of oleuropein. Oleuropein was previously extracted from olive leaves dried. Was obtained as yellow oil (70 % yield). DHPEA-EA(P) (methyl-4-(2-(3,4-dihydroxyphenethoxy)-2-oxoethyl)-3-formyl-2-methyl-3,4-dihydro-2H-pyran-5-carboxylate) peracetylated was obtained by catalytic acetylation [7]. Was obtained as a yellow solid (79 % yield).  $^1\text{H}$  and  $^{13}\text{C}$  NMR spectra of 3,4-DHPEA-EA and 3,4-DHPEA-EA (P) were in agreement with literature data [7].  $^1\text{H}$  and  $^{13}\text{C}$  NMR spectra were recorded at 300 and 75 MHz respectively in  $\text{CDCl}_3$  using tetramethylsilane (TMS) as internal standard on a Bruker ACP 300 MHz instrument.

The olive leaves, samples used for the extraction of oleuropein used to obtain 3,4-DHPEA-EA and 3,4-DHPEA-EA (P), were from *Coratina* cultivar of *Olea europaea*, collected from plants belonging to the olive grove of CREA, Research Centre for Olive, Citrus and TreeFruit, Rende, Cosenza, Italy, placed at 204 meters a.s.l. (39° 22' 17.681" N, 16° 13' 58.342" E). The sample dried for 48 h at 50 °C, milled, and kept at room temperature until use.

### 3. Results

#### 3.1 $\text{H}_2\text{O}_2$ reduces C2C12 myocytes viability and myogenesis

Studies reported in literature showed that  $\text{H}_2\text{O}_2$ , the most stable ROS, stimulates different biological responses in skeletal muscle ranging from physiological response to detrimental effects [30, 31]. In particular, high doses of  $\text{H}_2\text{O}_2$  reduced myocytes viability and impaired energetic metabolism [30-32]. Nevertheless, the molecular mechanism(s) that underlies the  $\text{H}_2\text{O}_2$ -induced alteration in intracellular redox state and cell viability of myocyte are still undefined.

Many molecules have been used to maintain, prevent or treat oxidative stress at skeletal muscle level, but in recent years a particular interest has turned towards the beneficial effects of oleuropein especially at muscular level. As previously mentioned, oleuropein has many biochemical functions including antimicrobial, anticancer and mainly antioxidant [33]. Despite these evidences the exact molecular mechanism that mediates the antioxidant effects of oleuropein in skeletal muscle is still little studied.

In the present work, we studied the effects of 3,4-DHPEA-EA(P), a oleuropein peracetylated derivative with several pharmacological functions [7], on C2C12 myocytes challenged with  $\text{H}_2\text{O}_2$ . To this aim C2C12 myocytes were differentiated for 2 days and treated with different concentration of  $\text{H}_2\text{O}_2$  for 24 h.

**Figure 1(A)** shows that  $\text{H}_2\text{O}_2$  significantly affects cell viability determined by MTS assay, in a concentration-dependent manner from 20  $\mu\text{M}$  to 100  $\mu\text{M}$ . Thus, the concentration of 100  $\mu\text{M}$   $\text{H}_2\text{O}_2$  was selected for following experiments. In order to deeply characterize this effect we performed a direct count of the cells upon Trypan blue staining at 24 h of treatment with 100  $\mu\text{M}$  of  $\text{H}_2\text{O}_2$ . **Figure 1(B)** shows that the number of viable cells was profoundly affected with a concomitant increase in dead cells (**Figure 1(C)**). These data were also confirmed by BrdU immunocytochemistry, which demonstrated a significant decrease in BrdU incorporation in  $\text{H}_2\text{O}_2$ -treated myocytes after 24 h, implying also a cell cycle arrest (**Figure 1(D)**). The  $\text{H}_2\text{O}_2$ -mediated cytotoxic effect was also established in terms of myogenesis. Indeed,  $\text{H}_2\text{O}_2$  treatment induced alteration in the differentiation program with an inhibition of MyoD expression (**Figure 1(E)**), a marker of the early stages of skeletal muscle differentiation [34]. To assess that the cytotoxic effect on the myocytes viability was due to  $\text{H}_2\text{O}_2$  we treated C2C12 cells with catalase, which scavengers  $\text{H}_2\text{O}_2$ . **Figure 1(B)** demonstrated that catalase treatment effectively counteracts  $\text{H}_2\text{O}_2$ -mediated decrease in the number of myocytes, the number of which was completely restored as in the untreated condition.

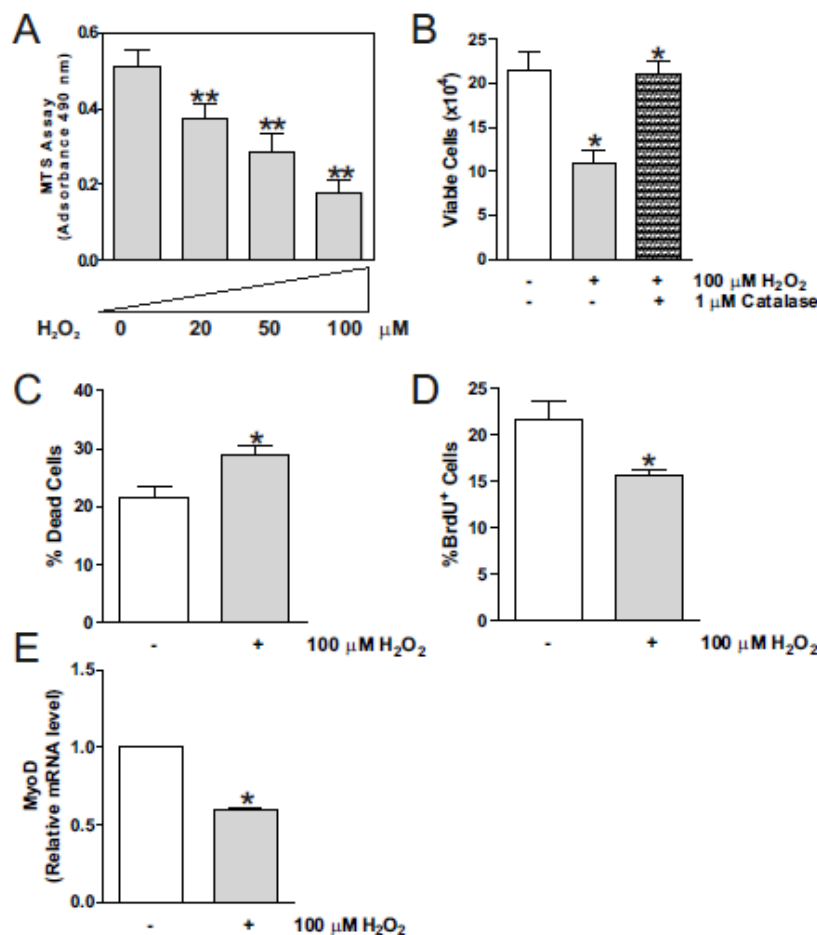


**Figure 1.** H<sub>2</sub>O<sub>2</sub> treatment induces a decrease in cell viability of murine C2C12 myocytes. C2C12 cells were differentiated in DM for 2 days. (A) At day 2 C2C12 myocytes were treated with H<sub>2</sub>O<sub>2</sub> (20, 50 and 100 μM) for 24 h. C2C12 myocytes viability was assayed by MTS. Data are expressed as means ± S.D. (n=8, \*\**p*<0.001). (B) C2C12 myocytes were treated with 100 μM H<sub>2</sub>O<sub>2</sub> for 24 h and viable cells were determined with Trypan Blue exclusion. 1 μM Catalase was added in culture medium 1 h prior H<sub>2</sub>O<sub>2</sub> and maintained throughout the experiment. Data are expressed as means ± S.D. (n=6, \**p*<0.01 vs Ctr cells). (C) C2C12 myocytes were treated with 100 μM H<sub>2</sub>O<sub>2</sub> for 24 h and dead cells were counted by Trypan Blue exclusion. Data are expressed as means ± S.D. (n=4, \**p*<0.01). (D) C2C12 myocytes were treated with 100 μM H<sub>2</sub>O<sub>2</sub> for 24 h and cells number was determined through immunofluorescence detection of incorporated BrdU. Data are expressed as means ± S.D. (n=4, \**p*<0.01). (E) Total RNA was isolated and relative mRNA level of MyoD was analyzed by RT-qPCR. Data are expressed as means ± S.D. (n=3, \**p*<0.01).

### 3.2. 3,4-DHPEA-EA(P) prevents the cytotoxic effect of H<sub>2</sub>O<sub>2</sub> in C2C12 myocytes

Next we tested whether oleuropein derivatives could function as antioxidant agent and mitigate H<sub>2</sub>O<sub>2</sub>-mediated cytotoxicity in C2C12 myocytes. To this end, C2C12 myocytes at day 2 of differentiation were pretreated with 10 μM 3,4-DHPEA-EA and 3,4-DHPEA-EA(P) for 1 h and subsequently with 100 μM H<sub>2</sub>O<sub>2</sub> for 24 h. **Figure 2(A)** shows that the two natural compounds are able to recover cell viability after treatment with H<sub>2</sub>O<sub>2</sub>, even though with different degrees of efficiency. Thus, we chose the compound which better re-established cell viability, i.e. 3,4-DHPEA-EA(P), for the subsequent experiments in order to highlight the molecular mechanism(s) that mediate the protective effect.

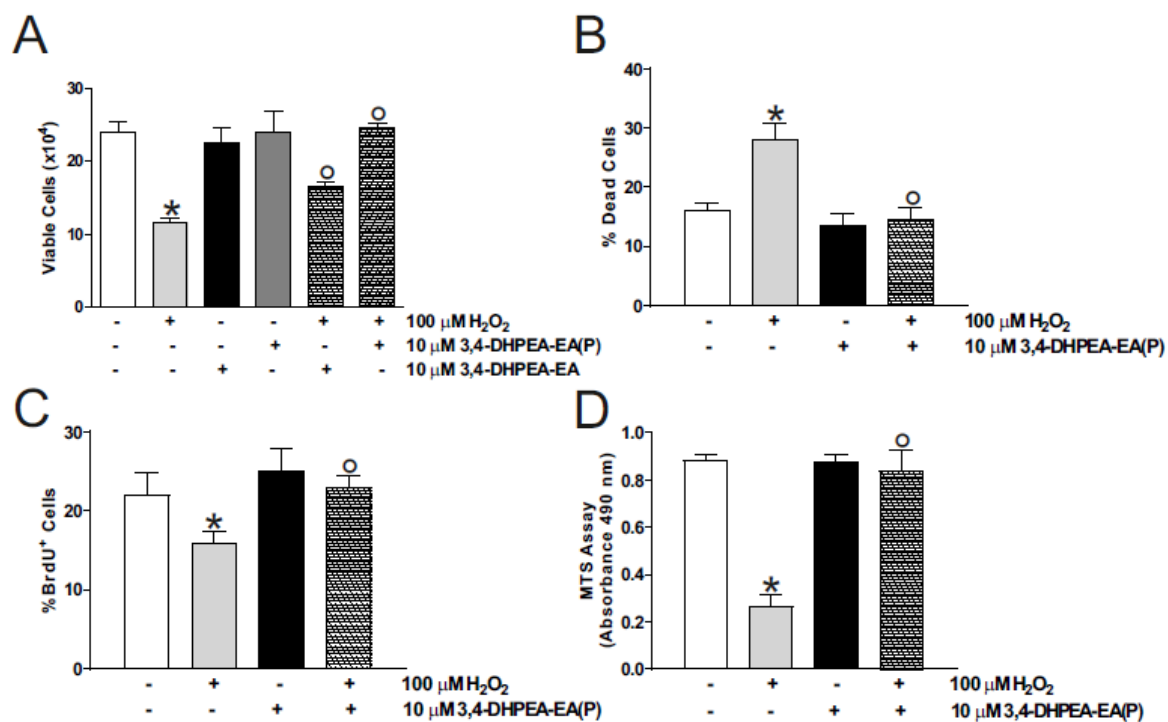


**Figure 2.** 3,4-DHPEA-EA(P) prevents growth arrest and cell death of H<sub>2</sub>O<sub>2</sub>-treated C2C12 myocytes. C2C12 cells were differentiated in DM for 2 days. At day 2 C2C12 myocytes were treated with H<sub>2</sub>O<sub>2</sub> (100 μM) for 24 h. (A) 3,4-DHPEA-EA and 3,4-DHPEA-EA(P) (10 μM) were added 1 h before H<sub>2</sub>O<sub>2</sub> treatment and maintained throughout the experiment. C2C12 myocytes were counted by Trypan Blue exclusion. Data are expressed as means ± S.D. (n=5, \**p*<0.01 vs Ctr cells; <sup>o</sup>*p*<0.01 vs H<sub>2</sub>O<sub>2</sub>-treated cells). (B) Dead cells were counted by Trypan Blue exclusion. Data are expressed as means ± S.D. (n=3, \**p*<0.01 vs Ctr cells; <sup>o</sup>*p*<0.01 vs H<sub>2</sub>O<sub>2</sub>-treated cells). (C) C2C12 myocytes cell viability was determined through immunofluorescence detection of incorporated BrdU. Data are expressed as means ± S.D. (n=3, \**p*<0.01 vs Ctr cells; <sup>o</sup>*p*<0.01 vs H<sub>2</sub>O<sub>2</sub>-treated cells). (D) C2C12 myocytes cell viability was assayed by MTS assay. Data are expressed as means ± S.D. (n=6, \**p*<0.01 vs Ctr cells; <sup>o</sup>*p*<0.01 vs H<sub>2</sub>O<sub>2</sub>-treated cells).

**Figure 2(B, C), and (D)** demonstrated that pre-treatment with 3,4-DHPEA-EA(P) was sufficient to counteract growth arrest and cell death elicited by H<sub>2</sub>O<sub>2</sub> treatment, as assessed through cell count by Trypan blue staining (**Figure 2(B)**) and BrdU incorporation (**Figure 2(C)**). The same result was obtained with MTS analysis (**Figure 2(D)**), confirming that 3,4-DHPEA-EA(P) exerted a protective effect against the H<sub>2</sub>O<sub>2</sub>-induced cytotoxicity.

### 3.3 3,4-DHPEA-EA(P) counteracts H<sub>2</sub>O<sub>2</sub>-mediate oxidative stress damage in C2C12 myocytes

Then we asked whether 3,4-DHPEA-EA(P) was able to counteract the deleterious effects of H<sub>2</sub>O<sub>2</sub> on C2C12 cell number by *buffering* intracellular ROS. The intracellular ROS levels were measured by means of cytofluorimetric analysis using the ROS-sensitive probe DCF-DA.

**Figure 3(A)** shows that 10 μM 3,4-DHPEA-EA(P) was able to lower the intracellular ROS content. In addition, we looked at the level of Ser139-phosphorylated histone H2A.X (pH2Ax), a hallmark of oxidative stress [35]. This analysis revealed that only nuclei of H<sub>2</sub>O<sub>2</sub>-treated C2C12 cells displayed an increase in pH2Ax protein content, which was efficiently reversed by 3,4-DHPEA-EA(P), indicating that DNA damage was caused by ROS imbalance (**Figure 3(B)**).

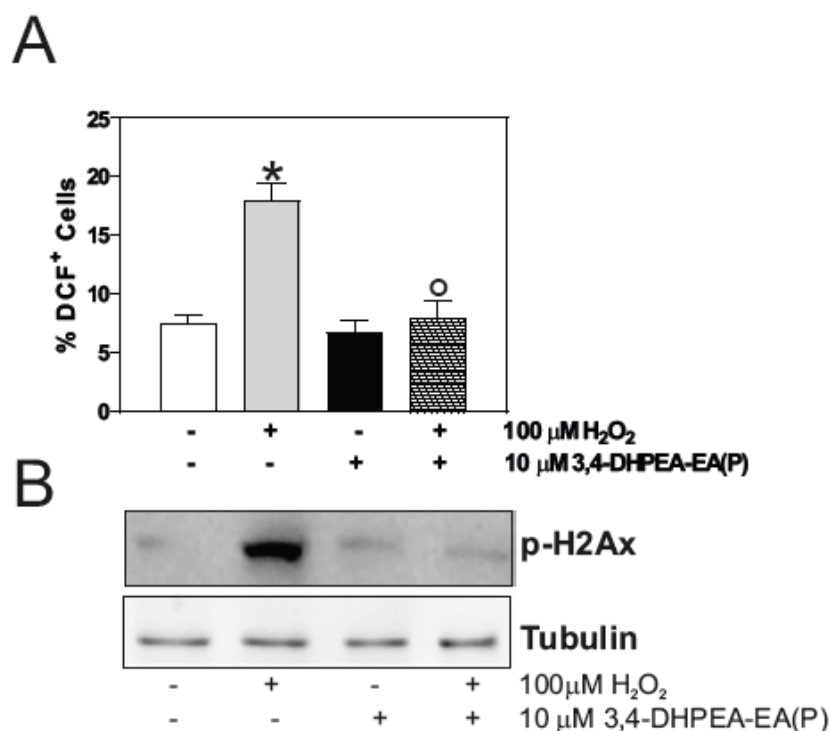


**Figure 3.** 3,4-DHPEA-EA(P) plays an antioxidant function in  $H_2O_2$ -treated C2C12 myocytes. C2C12 cells were differentiated in DM for 2 days. At day 2 C2C12 myocytes were treated with  $H_2O_2$  (100  $\mu$ M) for 24 h. 3,4-DHPEA-EA(P) (10  $\mu$ M) was added 1 h before  $H_2O_2$  treatment and maintained throughout the experiment. (A) C2C12 myocytes were incubated with DCF-DA for 1 h before the end of the experiments. ROS increase was evaluated measuring DCF fluorescence by cytofluorimetric analysis. Data are expressed as means  $\pm$  S.D. (n=3, \* $p$ <0.01 vs Ctr cells; <sup>o</sup> $p$ <0.01 vs  $H_2O_2$ -treated cells). (B) Cells were lysed and 20  $\mu$ g of proteins were loaded for Western blot analysis of p-H2Ax. Tubulin was used as loading control. All the immunoblots reported are from one experiment representative of four that gave similar results.

All these data suggest that 3,4-DHPEA-EA(P) exerts an antioxidant function under our experimental condition.

#### 3.4 3,4-DHPEA-EA(P) inhibits $H_2O_2$ -mediated decrease of C2C12 myocytes viability by inhibiting p-JNK signaling pathway

In understanding the mechanism(s) by which 3,4-DHPEA-EA(P) counteract the  $H_2O_2$ -induced growth arrest and cell death of myocytes, we focused on the stress-activated protein kinases c-Jun-N-terminal kinase (JNK) signaling pathway. In fact, it is known in the literature that JNK/MAPK signaling pathway is significantly downregulated during myogenesis, by negatively adjusting the differentiation of skeletal muscle cells [36]. Thus, we initially assessed whether 100  $\mu$ M  $H_2O_2$  was efficient in modulating the phospho-active form of JNK in our experimental system. We analyzed the protein content of p-JNK by Western blot analysis using a phospho-specific antibody. As showed in **Figure 4(A)** p-JNK was significantly increased after 24 h treatment with 100  $\mu$ M  $H_2O_2$  and 10  $\mu$ M 3,4-DHPEA-EA(P) efficiently counteracts this activation. We then attempted to delineate the JNK-pathway activated by  $H_2O_2$  treatment. Many reports demonstrated that c-Jun is among the transcription factors downstream JNK governing cell growth and survival [37].

As reported in **Figure 4(A)** p-c-Jun accumulated after  $H_2O_2$  treatment in C2C12 myocytes and also in this case the 3,4-DHPEA-EA(P) was able to significantly reduced the phosphorylation of p-c-Jun, suggesting that C2C12 growth arrest and cell dead proceeds *via* the JNK/c-Jun pathway.

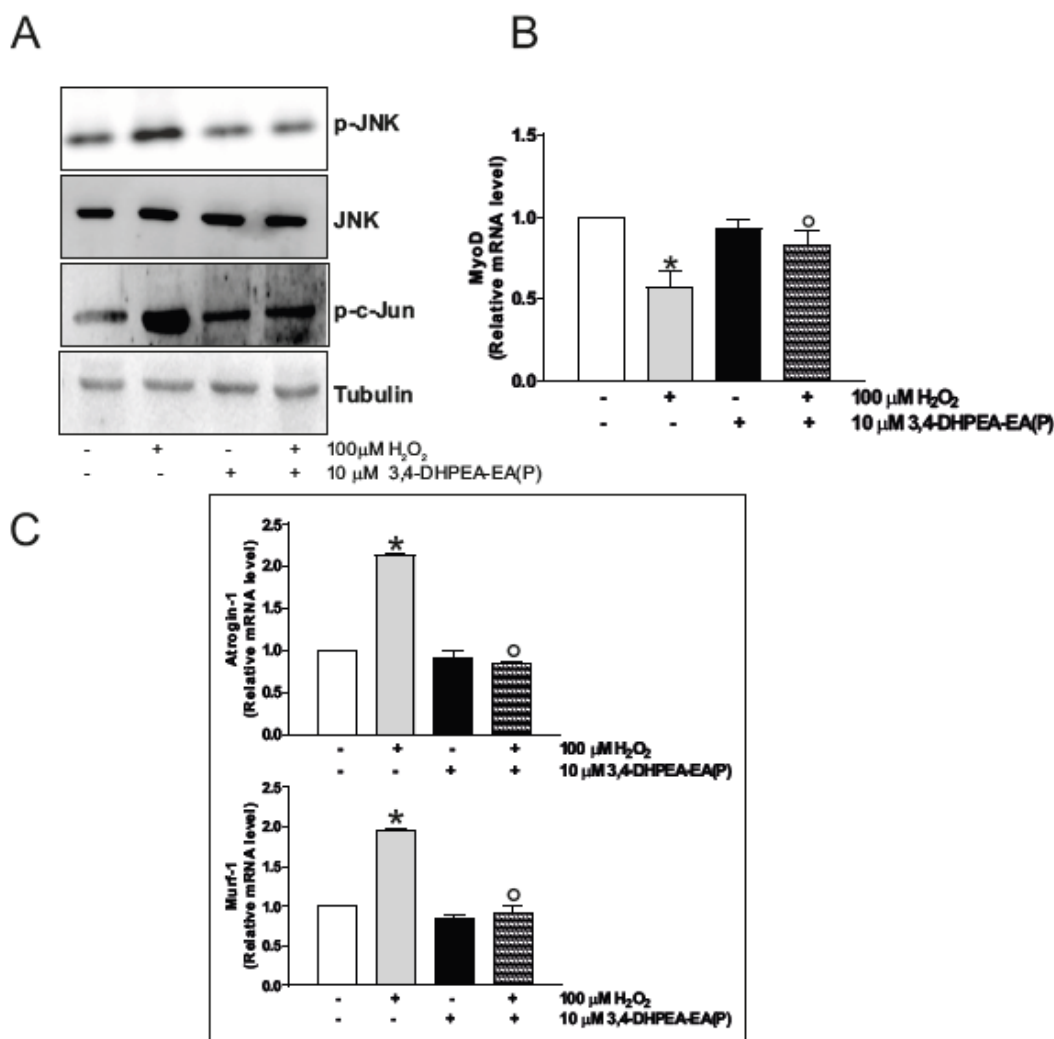


**Figure 4.** 3,4-DHPEA-EA(P) inhibits p-JNK/c-Jun axis and degeneration-related cellular molecular markers. C2C12 cells were differentiated in DM for 2 days. At day 2 C2C12 myocytes were treated with  $H_2O_2$  (100  $\mu$ M) for 24 h. 3,4-DHPEA-EA(P) (10  $\mu$ M) was added 1 h before  $H_2O_2$  treatment and maintained throughout the experiment. (A) Cells were lysed and 20  $\mu$ g of proteins were loaded for Western blot analysis of p-JNK, JNK, p-c-Jun. Tubulin was used as loading control. All the immunoblots reported are from one experiment representative of four that gave similar results. (B) Total RNA was isolated and relative mRNA level of MyoD was analyzed by RT-qPCR. Data are expressed as means  $\pm$  S.D. ( $n=3$ , \* $p<0.01$  vs Ctr cells;  $^o p<0.01$  vs  $H_2O_2$ -treated cells). (C) Total RNA was isolated and relative mRNA levels of Atrogin-1 and Murf-1 were analyzed by RT-qPCR. Data are expressed as means  $\pm$  S.D. ( $n=4$ , \* $p<0.01$  vs Ctr cells;  $^o p<0.01$  vs  $H_2O_2$ -treated cells).

### 3.5. 3,4-DHPEA-EA(P) prevents C2C12 atrophy mediated by $H_2O_2$ treatment

Finally, we checked the effect of 3,4-DHPEA-EA(P) on the myogenesis of C2C12 cells. **Figure 4(B)** shows that MyoD mRNA levels were significantly restored after treatment with 3,4-DHPEA-EA(P) with respect to  $H_2O_2$  treated myocytes, suggesting a complete restoration of the differentiation process. This hypothesis was further confirmed by the analyses of Atrogin-1 (F-box protein 32) and Murf-1 (tripartite motif-containing 63), molecular factors involved in the atrophy process as muscle-specific E3 ubiquitin ligase that are increased during skeletal muscle atrophy [38]. **Figure 4(C)** highlights a significant increase of their expression in  $H_2O_2$ -treated myocytes, suggesting that oxidative stress induced by  $H_2O_2$  not only blocks the differentiation process but also triggers a degenerative process. The pre-treatment with 3,4-DHPEA-EA(P) prevents the induction of atrophy-specific ubiquitin ligase suggesting that this molecule could modulate the integrity of skeletal muscle functioning as antioxidant.

#### 4. Discussion

Metabolic alterations of skeletal muscle are associated with pathologies such as sarcopenia, muscular dystrophies and atrophy. These conditions are characterized by an accumulation of oxidative damage that may contribute to loss of muscular tissue homeostasis. In healthy skeletal muscle, ROS are fundamental mediators of signaling pathways that have an impact on proliferation differentiation and apoptosis [39]. At low concentration ROS stimulate healing and maintenance of muscle [40], but if ROS levels is excessively high, it can delay tissue repair and even worsen the injury leading to atrophy [41]. To date, prevention/treatment to reduce oxidative stress under muscular atrophy or during increase in reactive species is not available. Nevertheless, antioxidants dietary supplementation was taken into consideration for the treatment of oxidative stress in the muscle as it is able to raise the levels of endogenous antioxidants or induce muscle repair [41, 42].

In this context, it has been demonstrated that oleuropein, the main polyphenol of olive oil, and its derivatives had antioxidant and anti-inflammatory proprieties in skeletal muscle. In particular, the treatment with hydroxytyrosol (HT) increases creatine kinase activity and myosin heavy chain expression, which are indicators of muscle cell differentiation and strength of contraction, respectively [43, 44]. Moreover, oleuropein derivatives attenuated the tumor necrosis factor- $\alpha$  (TNF- $\alpha$ )-induced downregulation of mitochondrial biogenesis by increasing peroxisome proliferator-activated receptor- $\gamma$  coactivator (PGC-1 $\alpha$ ), mitochondrial complexes (I and II) and myogenin expression [45]. This indicated that oleuropein improves mitochondrial development and function in muscle cells under inflammatory stress.

In this study we focused on the signaling pathways activated by H<sub>2</sub>O<sub>2</sub> treatment (used as model of oxidative stress) in C2C12 myocytes cell viability and differentiation. Our data demonstrated that high doses (100  $\mu$ M) of H<sub>2</sub>O<sub>2</sub> induce a significant inhibition of cell growth that resulted in myocytes death through the activation of the canonical p-JNK/p-c-Jun signaling pathway. H<sub>2</sub>O<sub>2</sub> toxicity was dose-dependent as already reported in the literature [31, 46, 47]. ROS production represents the earliest step in the scale of events occurring on H<sub>2</sub>O<sub>2</sub> treatment. The oxidative burst resulted in DNA damage as demonstrated by the phosphorylation of histone pH2Ax, which controls the recruitment of the DNA repair machinery in response to DNA strand break during replication [48]. The involvement of ROS-mediated damage during H<sub>2</sub>O<sub>2</sub> cytotoxic action on myocytes was confirmed by using treatment with the antioxidant catalase, which was able to efficiently abolish myocytes growth arrest. Furthermore, we showed that the oxidative burst is able to block the differentiation process of myocytes, as shown by the drop of MyoD expression. MyoD is a transcription factor implicated in the early stage of myogenic differentiation and necessary for the progression of quiescent muscle satellite cells in the cell cycle [49].

Moreover, tyrosol, a phenolic antioxidant present in the olive oil, was demonstrated to be effective in inhibiting H<sub>2</sub>O<sub>2</sub>-induced death of L6 muscle cells by regulating extracellular signal-regulated kinases (ERK), JNK and p38 MAPK [50]. Our findings reveal that 3,4-DHPEA-EA(P), a bioactive compounds present in olive leaves, suppressed H<sub>2</sub>O<sub>2</sub>-mediated cytotoxicity in C2C12 myocytes already at a concentration of 10  $\mu$ M with a significant increase in the viability. Moreover, our results showed that 3,4-DHPEA-EA(P) treatment promotes the myogenesis process by restoring the expression of MyoD in H<sub>2</sub>O<sub>2</sub>-treated C2C12 myocytes.

Among redox-sensitive factors able to modulate myocytes cycle progression and differentiation, MAPK are known to be activated in response to ROS production. In particular, it is known that p-JNK-p-c-Jun MAPK are negative regulators of myogenesis playing a role opposite to that of p38 during differentiation [36], which instead is considered a pro-myogenic factor [51]. In accordance, we found that H<sub>2</sub>O<sub>2</sub>-induced oxidative stress activates the redox-sensitive p-JNK-c-Jun pathway exerting a pro-apoptotic role in muscle cells. Antioxidant treatment with 3,4-DHPEA-EA(P) not only restored redox balance but also inhibits p-JNK-c-Jun activation and phosphorylation improving cell viability and differentiation of C2C12 myocytes.

As previously mentioned an accumulation of oxidative damage could contribute to loss of muscular homeostasis, function and atrophy. Interestingly we have shown that the increase of oxidative stress is associated with increased marker of myotube atrophy implying the occurrence of

a degenerative process upon oxidative stress conditions. In contrast 3,4-DHPEA-EA(P) treatment prevents the process of muscle degeneration suggesting the potential use of this molecule in conditions of high oxidative stress (i.e. physical exercise, sarcopenia and aging) or during atrophy.

To conclude, our study highlights the antioxidant role of 3,4-DHPEA-EA(P) in C2C12 cells, as it is able to reduce intracellular levels of ROS resulting in inhibition of cell death and atrophy, conditions observed under increased oxidative stress. Future studies should be carried out to better clarify the effects of 3,4-DHPEA-EA(P) at cellular level and in vivo models to develop new therapeutic strategies for the treatment of muscular diseases related to the increase of oxidative stress.

**Author Contributions:** M.N. conceived and designed the experiments; S.B. performed the experiments; S.B. and M.R.C. analyzed the data; M.N. and P.C. synthesized and characterized 3,4-DHPEA-EA peracetylated; M.N. and S.B. wrote the paper. M.R.C. revised the manuscript. C.C. and A.P. performed the experiments. All authors read and approved the final manuscript.

**Funding:** This research received no external funding.

**Acknowledgments:** In this section you can acknowledge any support given which is not covered by the author contribution or funding sections. This may include administrative and technical support, or donations in kind (e.g., materials used for experiments).

**Conflicts of Interest:** The authors declare no conflict of interest.

## References

1. Barraji3n-Catal3n, E.; Taamalli, A.; Quirantes-Pin3, R.; Roldan-Segura, C.; Arr3ez-Rom3n, D.; Segura-Carretero, A.; Micol, V.; Zarrouk, M. Differential metabolomic analysis of the potential antiproliferative mechanism of olive leaf extract on the JIMT-1 breast cancer cell line. *J Pharm Biomed Anal*, **2015**, *105*, 156-62.
2. Bulotta, S.; Cellano, M.; Lepore, S.M.; Montalcini, T.; Puija, A.; Russo, D. Beneficial effects of the olive oil phenolic components oleuropein and hydroxytyrosol: focus on protection against cardiovascular and metabolic diseases. *J Transl Med*, **2014**, *12*,219, 1-9
3. Visioli, F. and C. Galli, Antiatherogenic components of olive oil. *Curr Atheroscler Rep*, 2001. **3**(1): p. 64-67.
4. Impellizzeri, D.; Esposito, E.; Mazzon, E.; Paterniti, I.; Di Paola, R.; Bramanti, P.; Morittu, V.M.; Procopio, A.; Britti, D.; Cuzzocrea, S. The effects of oleuropein aglycone, an olive oil compound, in a mouse model of carrageenan-induced pleurisy. *Clin Nutr*, **2011**, *30*(4), 533-540.
5. Impellizzeri, D.; Esposito, E.; Mazzon, E.; Paterniti, I.; Di Paola, R.; Bramanti, P.; Morittu, V.M.; Procopio, A.; Britti, D.; Cuzzocrea, S. Oleuropein aglycone, an olive oil compound, ameliorates development of arthritis caused by injection of collagen type II in mice. *J Pharmacol Exp Ther*, **2011**, *339*(3), 859-869.
6. Pantano, D.; Luccarini, I.; Nardiello, P.; Servili, M.; Stefani, M.; Casamenti, F. Oleuropein aglycone and polyphenols from olive mill waste water ameliorate cognitive deficits and neuropathology. *Br J Clin Pharmacol*, **2017**, *83*(1), 54-62.
7. Procopio, A.; Alcaro, S.; Nardi, M.; Oliverio, M.; Ortuso, F.; Sacchetta, P.; Pieragostino, P.; Sindona, G. Synthesis, biological evaluation, and molecular modeling of oleuropein and its semisynthetic derivatives as cyclooxygenase inhibitors. Synthesis, biological evaluation, and molecular modeling of oleuropein and its semisynthetic derivatives as cyclooxygenase inhibitors. *J Agric Food Chem*, **2009**, *57*(23), 11161-11167.
8. Bonacci, S., Paonessa, R.; Costanzo, P.; Salerno, R.; Maiuolo, J.; Nardi, M.; Procopio, A.; Oliverio, M. Peracetylation as a strategy to improve oleuropein stability and its affinity to fatty foods. *Food Funct*, **2018**, *9*(11), 5759-5767.

9. Nardi, M.; Bonacci, S.; Cariati, L.; Costanzo, P.; Oliverio, M.; Sindona, G.; Procopio, A. Synthesis and antioxidant evaluation of lipophilic oleuropein aglycone derivatives *Food Funct*, **2017**, *8*(12), 4684-4692.
10. Sindona G., Caruso A., Cozza A., Fiorentini S., Lorusso B., Marini E., Nardi M., Procopio A., Zicari S. *Current Med Chem*, **2012**, *19*, 4006-4013.
11. Nardi, M., Bonacci, S., De Luca, G., Maiuolo, J., Oliverio, M., Sindona, G., Procopio, A. Biomimetic synthesis and antioxidant evaluation of 3,4-DHPEA-EDA [2-(3,4-hydroxyphenyl) ethyl (3S,4E)-4-formyl-3-(2-oxoethyl)hex-4-enoate]. *Food Chem* **2014**, *162*, 89-93.
12. Fujiwara, Y.; Tsukahara, C.; Ikeda, N.; Sone, Y.; Ishikawa, T.; Ichi, I.; Koike, T.; Aoki, Y. Oleuropein improves insulin resistance in skeletal muscle by promoting the translocation of GLUT4. *J Clin Biochem Nutr*, **2017**. *61*(3), 196-202.
13. Alkhateeb, H.; Al-Duais, M.; Qnais, E. Beneficial effects of oleuropein on glucose uptake and on parameters relevant to the normal homeostatic mechanisms of glucose regulation in rat skeletal muscle. *Phytother Res*, **2018**. *32*(4), 651-656.
14. Rodriguez, V.M.; Portillo, M.P.; Pico, C.; Macarulla, M.T.; Palou, A. Olive oil feeding up-regulates uncoupling protein genes in rat brown adipose tissue and skeletal muscle. *Am J Clin Nutr*, **2002**. *75*(2), 213-220.
15. Baldelli, S.; Ciccarone, F.; Limongi, D.; Checconi, P.; Palmara, A.T.; Ciriolo, M. R. Glutathione and Nitric Oxide: Key Team Players in Use and Disuse of Skeletal Muscle. *Nutrients*, **2019**. *11*(10), 1-8.
16. Powers, S.K.; Ji, L.L.; Kavazis, A.N.; Jackson, M.J. Reactive oxygen species: impact on skeletal muscle. *Compr Physiol*, **2011**. *1*(2), 941-969.
17. Powers, S.K.; Jackson, M.J. Exercise-induced oxidative stress: cellular mechanisms and impact on muscle force production. *Physiol Rev*, **2008**. *88*(4), 1243-1276.
18. Fulle, S.; Protasi, F.; Di Tano, G.; Pietrangelo, T.; Beltramin, A.; Boncompagni, S.; Vecchiet, L.; Fanò, G. The contribution of reactive oxygen species to sarcopenia and muscle ageing. *Exp Gerontol*, **2004**. *39*(1), 17-24.
19. Muller, F.L.; Song, W.; Jang, Y.C.; Liu, Y.; Sabia, M.; Richardson, A.; Van Remmen, H. Denervation-induced skeletal muscle atrophy is associated with increased mitochondrial ROS production. *Am J Physiol Regul Integr Comp Physiol*, **2007**. *293*(3), R1159-1168.
20. Muhammad, M.H.; Allam, M.M. Resveratrol and/or exercise training counteract aging-associated decline of physical endurance in aged mice; targeting mitochondrial biogenesis and function. *J Physiol Sci*, **2018**. *68*(5), 681-688.
21. Pierno, S.; Tricarico, D.; Liantonio, A.; Mele, A.; Digennaro, C.; Rolland, J. F.; Bianco, G.; Villanova, L.; Marendino, A.; Camerino, G.; De Luca, A.; Desaphy, F. F.; Camerino, D. C. An olive oil-derived antioxidant mixture ameliorates the age-related decline of skeletal muscle function. *Age (Dordr)*, **2014**. *36*(1), 73-88.
22. Hadrich, F., Garcia, M.; Maalej, A.; Moldes, M.; Isoda, H.; Feve, B.; Sayadi, S. Oleuropein activated AMPK and induced insulin sensitivity in C2C12 muscle cells. *Life Sci*, **2016**. *151*, 167-173.
23. Shen, Y., Song, S. J.; Keum, N.; Park, T. Olive leaf extract attenuates obesity in high-fat diet-fed mice by modulating the expression of molecules involved in adipogenesis and thermogenesis. *Evid Based Complement Alternat Med*, **2014**, 971890, 1-12.
24. Cao, K.; Xu, J.; Zou, X.; Li, Y.; Chen, C.; Zheng, A.; Li, H.; Szeto, I. M. Y.; Shi, Y.; Long.; Liu, J.; Feng, Z. Hydroxytyrosol prevents diet-induced metabolic syndrome and attenuates mitochondrial abnormalities in obese mice. *Free Radic Biol Med*, **2014**. *67*, 396-407.

25. Aquilano, K.; Baldelli, S.; La Barbera, L.; Lettieri Barbato, D.; Tatulli, G.; Ciriolo, M. R. Adipose triglyceride lipase decrement affects skeletal muscle homeostasis during aging through FAs-PPARalpha-PGC-1alpha antioxidant response. *Oncotarget*, **2016**, 7(17), 23019-23032.
26. Baldelli, S.; Aquilano, K.; Rotilio, G.; Ciriolo, M. R. Glutathione and copper, zinc superoxide dismutase are modulated by overexpression of neuronal nitric oxide synthase. *Int J Biochem Cell Biol*, **2008**, 40(11), 2660-2670.
27. Pagliei, B.; Aquilano, K.; Baldelli, S.; Ciriolo, M. R. Garlic-derived diallyl disulfide modulates peroxisome proliferator activated receptor gamma co-activator 1 alpha in neuroblastoma cells. *Biochem Pharmacol*, **2013**, 85(3), 335-344.
28. Baldelli, S. ; Ciriolo, M.R. Altered S-nitrosylation of p53 is responsible for impaired antioxidant response in skeletal muscle during aging. *Aging (Albany NY)*, **2016**, 8(12), 3450-3467.
29. Lowry, O.H.; Rosebrough, N. J.; Farr, A. L.; Bandall, R. J. Protein measurement with the Folin phenol reagent. *J Biol Chem*, **1951**, 193(1), 265-275.
30. Bosutti, A.; Degens, H. The impact of resveratrol and hydrogen peroxide on muscle cell plasticity shows a dose-dependent interaction (vol 5, 8093, 2015). *Scientific Reports*, **2015**, 5, 1-13
31. Siu, P.M.; Y. Wang, and S.E. Alway, Apoptotic signaling induced by H<sub>2</sub>O<sub>2</sub>-mediated oxidative stress in differentiated C2C12 myotubes. *Life Sci*, **2009**, 84(13-14), 468-481.
32. Caporossi, D.; Ciaffrè, S. A.; Pittaluga, M.; Farace, M. G. Cellular responses to H<sub>2</sub>O<sub>2</sub> and bleomycin-induced oxidative stress in L6C5 rat myoblasts. *Free Radical Bio. Med.* **2003**, 35(11), 1355-1364.
33. Barbaro, B.; Toietta, G.; Maggio, R.; Arciello, M.; Tarocchi, M.; Galli, A.; Balsano, C. Effects of the olive-derived polyphenol oleuropein on human health. *Int J Mol Sci*, **2014**, 15(10), 18508-24.
34. Wilson, E.M.; Rotwein, P. Control of MyoD function during initiation of muscle differentiation by an autocrine signaling pathway activated by insulin-like growth factor-II. *J Bio Chem*, **2006**, 281(40), 29962-29971.
35. Aquilano, K.; Baldelli, S.; Cardaci, S.; Rotilio, G.; Ciriolo, M. R. Nitric oxide is the primary mediator of cytotoxicity induced by GSH depletion in neuronal cells. *J. Cell Sci*, **2011**, 124(7), 1043-1054.
36. Xie, S.J.; Li, J. H.; Chen, H. F.; Tan, Y. Y.; Liu, S. R.; Zheng, L.L.; Huang, M.B.; Guo, Y. H.; Zhang, Q.; Zhou, H.; Qu, L.H. Inhibition of the JNK/MAPK signaling pathway by myogenesis-associated miRNAs is required for skeletal muscle development. *Cell Death Differ*, **2018**, 25(9), 1581-1597.
37. Bogoyevitch, M.A.; Kobe, B. Uses for JNK: the many and varied substrates of the c-Jun N-terminal kinases. *Microbiol Mol Biol Rev*, **2006**, 70(4), 1061-1095.
38. Baldelli, S.; Ciriolo, M.R. Altered S-nitrosylation of p53 is responsible for impaired antioxidant response in skeletal muscle during aging. *Aging-U.S*, **2016**, 8(12), 3450-3462.
39. Michaelson, L.P.; Iler, C.; Ward, C.W. ROS and RNS signaling in skeletal muscle: critical signals and therapeutic targets. *Annu Rev Nurs Res*, **2013**, 31, 367-387.
40. Powers, S.K.; Talbert, E.E.; Adhietty, P.J. Reactive oxygen and nitrogen species as intracellular signals in skeletal muscle. *J Physiol*, **2011**, 589(Pt 9), 2129-2138.
41. Valko, M.; Leibfritz, D.; Moncol, J.; Cronin, M. T.D.; Mazur, M.; Telser, J. Free radicals and antioxidants in normal physiological functions and human disease. *Int J Biochem Cell Biol*, **2007**, 39(1), 44-84.
42. McCalley, A.E.; Kaja, S.; Payne, A. J.; Koulen, P. Resveratrol and calcium signaling: molecular mechanisms and clinical relevance. *Molecules*, **2014**, 19(6), 7327-7340.
43. Burattini, S.; Anti-apoptotic activity of hydroxytyrosol and hydroxytyrosyl laurate. *Food Chem Toxicol*, **2013**, 55, 248-256.

44. Vlavecshi, F.; Young, M.; Tsiani, E. Antidiabetic Effects of Hydroxytyrosol: In Vitro and In Vivo Evidence. *Antioxidants* (Basel), **2019**, *8*(6), 1-20.
45. Kikusato, M.; Muroi, H.; Uwabe, Y.; Furukawa, K.; Toyomuzu, M. Oleuropein induces mitochondrial biogenesis and decreases reactive oxygen species generation in cultured avian muscle cells, possibly via an up-regulation of peroxisome proliferator-activated receptor gamma coactivator-1alpha. *Anim Sci J*, **2016**, *87*(11), 1371-1378.
46. Kim, H.; Lee, K. II.; Jang, M.; Namkoong, S.; Park, R.; Ju, H.; Choi, I.; Oh, W. K.; Park, J. Conessine Interferes with Oxidative Stress-Induced C2C12 Myoblast Cell Death through Inhibition of Autophagic Flux. *PLoS One*, **2016**, *11*(6): p. e0157096, 1-9.
47. Santa-Gonzalez, G.A.; Gomez-Molina, A.; Arcos-Burgos M.; Meyer, J.N.; Camargo, M. Distinctive adaptive response to repeated exposure to hydrogen peroxide associated with upregulation of DNA repair genes and cell cycle arrest. *Redox Biol*, **2016**, *9*, 124-133
48. Sharma, A.; Singh, K.; Almasan, A. Histone H2AX phosphorylation: a marker for DNA damage. *Methods Mol Biol*, **2012**, *920*, 613-626.
49. Berkes, C.A.; Tapscott, S.J.; MyoD and the transcriptional control of myogenesis. *Semin Cell Dev Biol*, **2005**, *16*(4-5): p. 585-595.
50. Karkovic Markovic, A.; Toric, J.; Barbaric, M.; Brala, C. J. Hydroxytyrosol, Tyrosol and Derivatives and Their Potential Effects on Human Health. *Molecules*, **2019**, *24*(10), 17-24
51. Wu, Z.; Woodring, P.J.; Bhakta, K.S.; Tamura, K.; Wen, F.; Feramisco, J.R.; Karin, M.; Wang, J.Y.; Puri, P.L. p38 and extracellular signal-regulated kinases regulate the myogenic program at multiple steps. *Mol Cell Biol*, **2000**, *20*(11): 3951-64.